

Supplementary Material and Methods

Cell culture. HEK293T cells were maintained in DMEM high glucose supplemented with 10% fetal bovine serum (Gibco), penicillin (50 U/ml, Life Technology), and streptomycin (50 µg/ml, Life Technology). For stable cell lines, cells were transfected with lenti-viral shRNA to silence human endogenous RKIP, followed by puromycin selection (0.2 µg/ml) for one week. Then rat wild type RKIP or RKIP mutants were transiently transfected using the *TransIT*-LT1 transfection reagent (Mirus) and OPTI-MEM (Gibco).

RKIP mutations. RKIP mutants (S153A/K157A, S153A/K157E, S153E/K157E, D134A/E135A/S153A) were generated using a QuikChange II site-directed mutagenesis kit (Agilent Technologies) with a wild type (WT) RKIP carrying a HA tag in the pCDNA3.1 vector. All of the RKIP mutants generated were sequence validated at the University of Chicago Comprehensive Cancer Center (cancer-seqbase.uchicago.edu).

Antibodies and Chemicals. GRK2 (sc-13143, Santa Cruz), RKIP (sc-5423, Santa Cruz), HA high affinity (Roche), alpha tubulin (sc-8035, Santa Cruz) and Normal IgG (sc-2027, Santa Cruz) were used for *in vivo* protein analyses. Phorbol 12-myristate 13-acetate (PMA) was purchased from Sigma.

Co-immunoprecipitation (CoIP) assays. HEK293T-shRKIP cells (1×10^6) were transiently transfected for exogenous expression of wild type (WT) and mutant rat RKIP-HA tag along with a GRK2 expressing plasmid (2 µg). Transfected cells were followed by serum starvation overnight and treated for PMA (0.1 µM) for 10 min before collection of lysates in IP buffers (50 mM Tris pH 7.5, 150 mM NaCl, 0.25% Na-deoxycholate, 1% NP40, 1 mM EDTA) containing a protease inhibitor cocktail (Millipore) and phosphatase inhibitors (Goldbiosystem). Sonicated cell lysates were centrifuged at 11,000 *g* for 30 minutes at 4 °C and incubated with 25% protein G-sepharose 4 fast flow (GE Healthcare) with rabbit IgG for 1 hour at 4 °C to block non-specific binding with 25% G-sepharose. Precleared supernatants were precipitated using anti-HA antibody overnight at 4 °C followed by incubation with 25% G-

shearose. Anti-HA immunoprecipitated proteins were assayed for GRK2 blotting on nitrocellulose membrane (Amersham Hybond ECL). Bands in the western blots were detected and quantified using Li-Cor Image studio.

Protein purification for crystallization. cDNAs coding for N-terminal His₆-tagged WT mouse RKIP (His-RKIP) and the rat RKIP variant (His-RKIP^{Δ143-146}) were cloned into the expression vector pET3c (Novagen). His-RKIP and the RKIP variants were expressed in *Escherichia coli* BL21(DE3)pLysS cells. For purification of His-RKIP and the His-RKIP^{Δ143-146} variant the bacteria were thawed, resuspended and lysed in 50 mM Tris pH 7.4, 500 mM NaCl and 20 mM imidazole. The soluble fraction of the cell lysate was loaded onto a Ni Sepharose affinity column (Histrap, GE Healthcare/ ÄKTA), and eluted with a gradient to 500 mM imidazole (20 column volumes). The proteins were further purified by SEC (Superdex 200 26/60, GE Healthcare/ ÄKTA) in 20 mM PIPES pH 6.5, 150 mM NaCl and 1 mM EDTA. The protein samples were concentrated to up to 40 mg/ml, flash-frozen in liquid nitrogen and stored at -80°C.

Crystallization, Data collection and Structure Determination. 1 µl of WT RKIP at a concentration of 11 mg/ml in ddH₂O was mixed with 1 µl of the reservoir solution containing 25% PEG 6000 and 100 mM NaAcetate pH 4.6. The mixture was equilibrated in hanging drop vapor diffusion experiments at 20 °C against 1 ml of the reservoir solution. Crystals were flash frozen in liquid nitrogen utilizing mother liquor supplemented with 20% glycerol and data collection was performed at 100 K. The WT RKIP dataset was collected at beamline MX 14.1 (Bessy, Berlin).

His-RKIP^{Δ143-146} was crystallized at a protein concentration of 15 mg/ml in a buffer containing 150 mM NaCl and 100 mM NaAcetate. 1 µl of the protein solution was mixed with 1 µl of the reservoir and the mixture was equilibrated in hanging drop vapor diffusion experiments at 20 °C against 1 ml of the reservoir solution, containing 17.5% PEG3350 and 100 mM NaF. Crystals were flash frozen in liquid nitrogen utilizing mother liquor supplemented with 20% glycerol and data collection was

performed at 100 K, and processed with iMOSFLM (44, 45). The dataset of the His-RKIP^{Δ143-146} variant was collected at beamline MX 14.1 (Bessy, Berlin).

The structure of the WT protein was solved by molecular replacement using the program Phaser (46) and the structure of rat RKIP as a search model (pdb entry 2IQY). WT RKIP was refined with REFMAC5 (47, 48) and adjusted with Coot (49) incorporating anisotropic B-factor refinement. The structure of the His-RKIP^{Δ143-146} variant was solved by molecular replacement with MOLREP (50) using the WT protein as search model and was refined with REFMAC5 (47). Structures of RKIP (6ENS) and the Δ143-146 variant (6ENT) were deposited in the Protein Data Bank.

Multi-angle light scattering (MALS). Studies of the oligomeric state used MALS coupled with SEC and were conducted with a Wyatt DAWN Heleos II Static Light Scattering unit and a WTC-05S5 column (100 Å pore size, 100-100,000 MW range) at room temperature.

Methods for the algorithms and analyses.

Blast algorithm:

All multiple sequence alignments (MSA) are extracted from UniProt BLAST(51, 52):

<http://www.uniprot.org/blast/> with parameters as follows:

target DB | E-value | Matrix | Filtering | Gapped | TopHits

UniProtKB | 0.001 | BLOS-62 | Filter_Low | Gap_Yes | 1000_Hits

Select TopHits:

We extract top 500 sequences according to the ranking order of the Bit Scores (or, E-values). It should be noted that a high Bit Score or low E-value would indicate high sequence identity to the query sequence.

Multiple Sequence Alignment

We run Mafft (53) for these top 500 sequences to generate the final multiple sequence

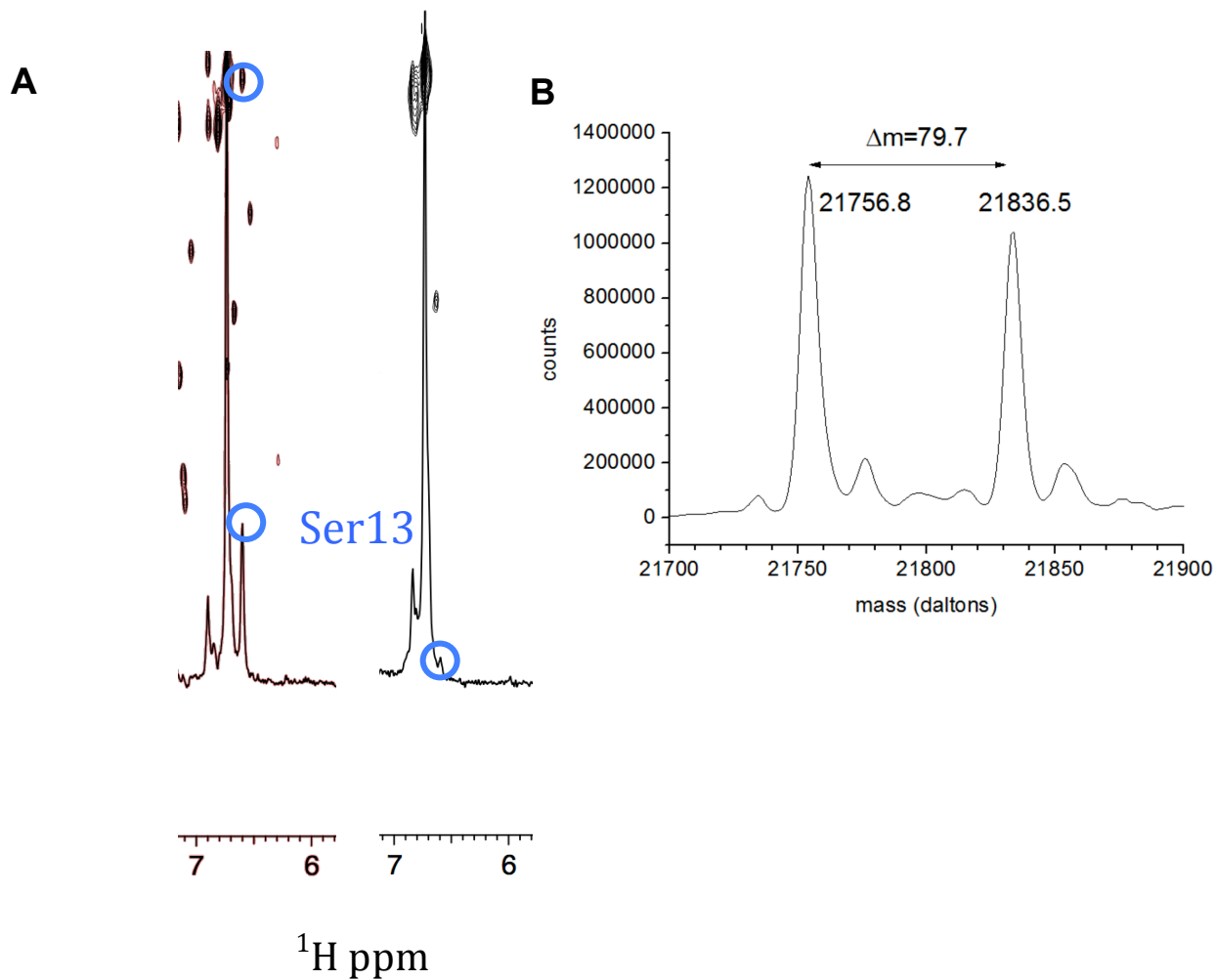
alignment (MSA).

<http://www.ebi.ac.uk/Tools/msa/mafft/>

Statistics

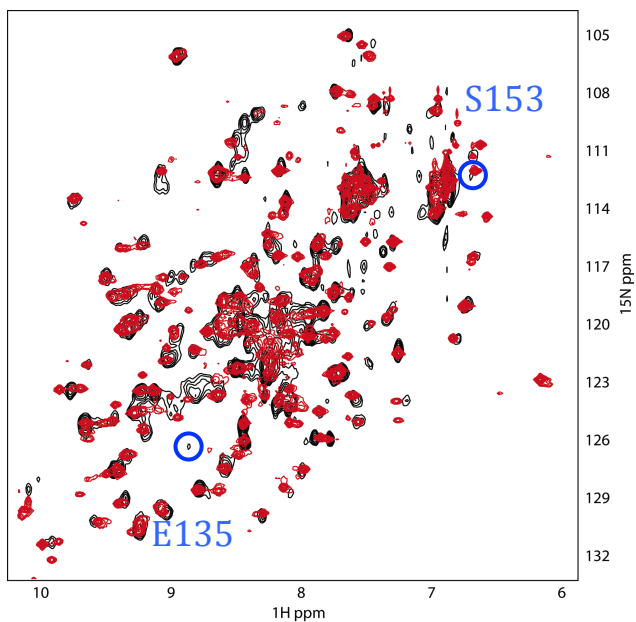
The errors listed for Supplementary Tables 2 and 3, and Figure 4A are the standard deviations calculated assuming a binomial distribution.

Supplementary Figures S1-S5 and Tables S1-S7

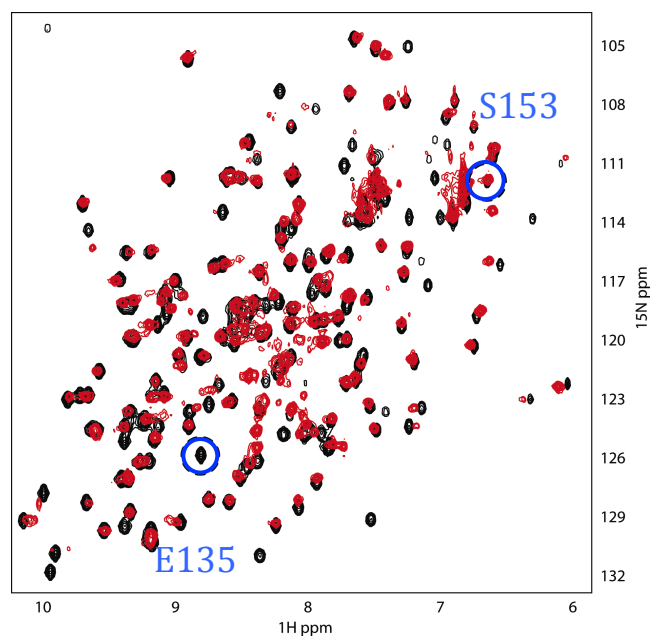


Supplementary Figure S1. Phosphorylation of S153. (A) Decrease in S153 NMR peak height due to phosphorylation (overlaid on the HSQC) **(B)** Mass spectrum of RKIP during phosphorylation process showing appropriate mass change (theoretical 80.0 daltons).

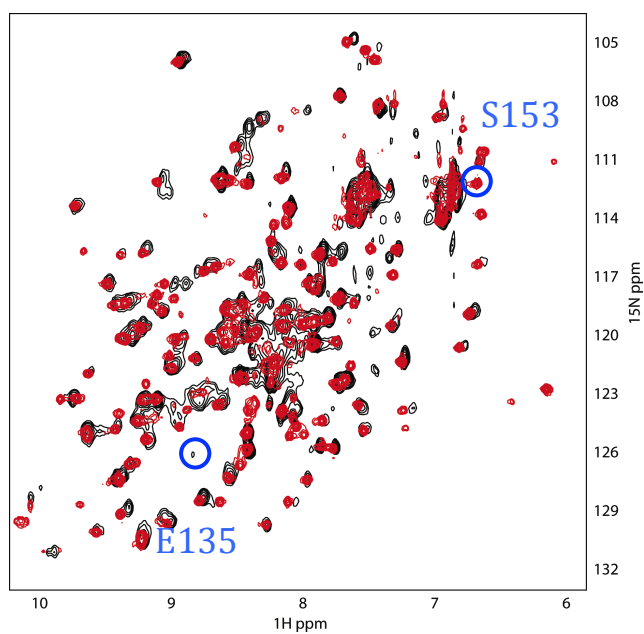
pS153,P74L versus K157E



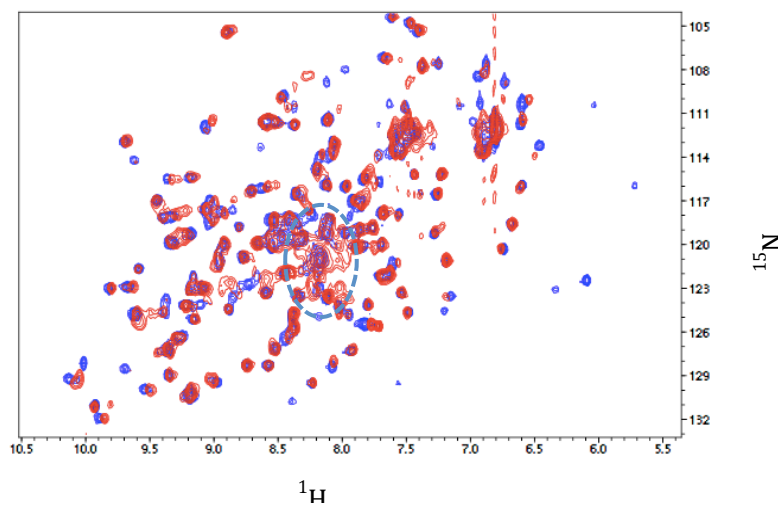
WT versus D134Y,E135Y



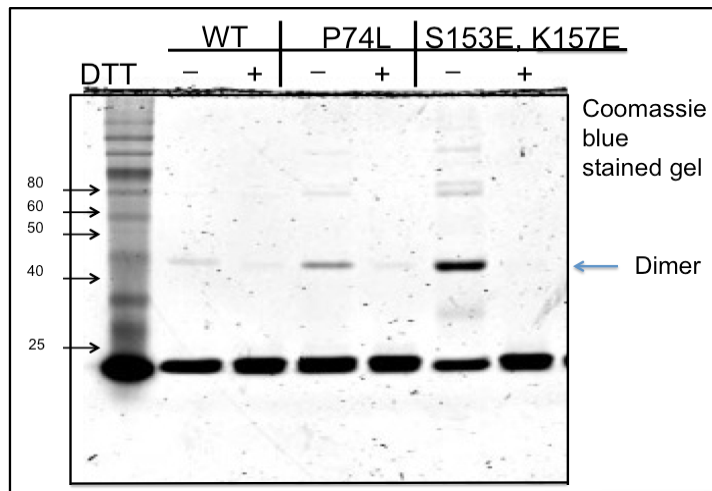
pS153,P74L versus D134Y,E157Y



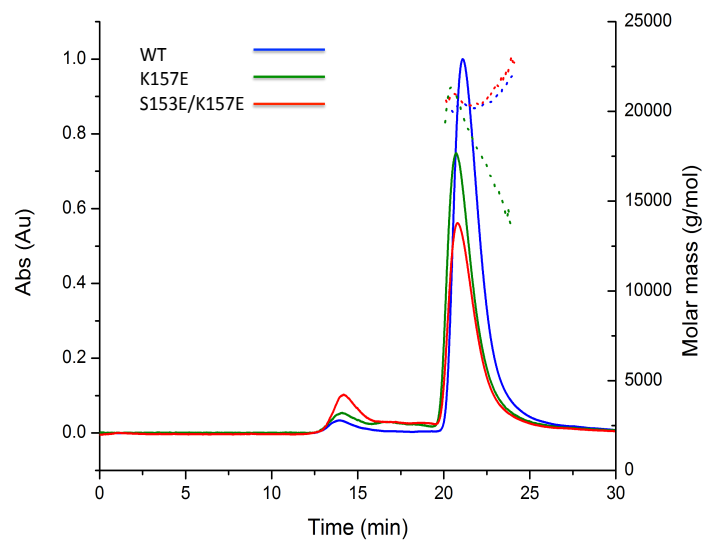
K157A versus K157E



Supplementary Figure S2. Comparison of ^{15}N - ^1H HSQC spectra at 25°C. The random coil region is highlighted (blue dashed circle).

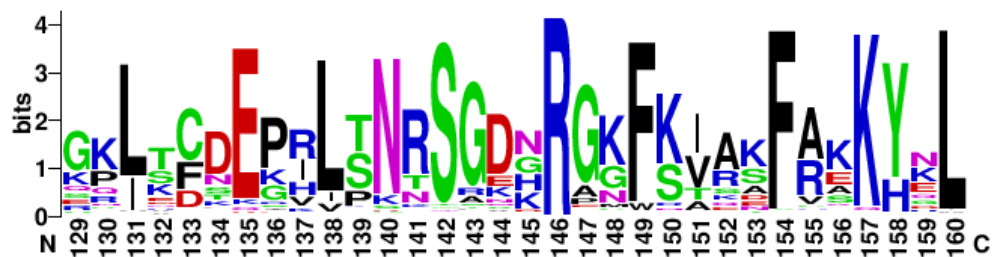


Supplementary Figure S3. Formation of RKIP oligomers is sensitive to reducing agents. Lysates from cells transfected with WT, P74L or S153E, K157E RKIP variants were boiled in the presence or absence of DTT. Samples were resolved by SDS PAGE and stained with Coomassie blue.

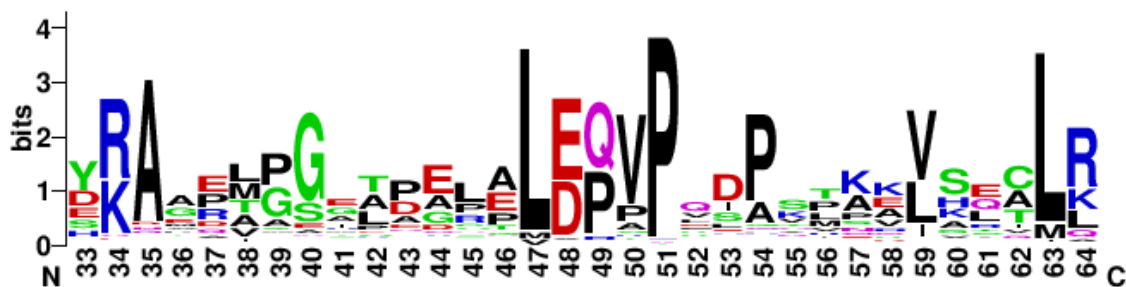


Supplementary Figure S4. Multi-angle light scattering (MALS) data indicating that RKIP is monomeric under reducing conditions. The small, high molecular weight peak observed by scattering did not exhibit UV absorbance (dotted line), suggesting that it is not proteinaceous.

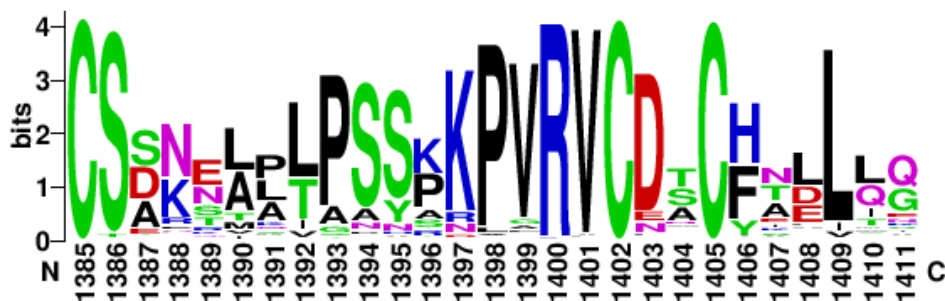
a) RKIP (S153 and K157)



b) Bax (S60 and K64)



c) EEA1 (T1392 and K1396)



d) Troponin I (S42 and K46)



Supplementary Figure S5. Conserved Residues in Proteins with a Phosphotheft Motif. (a) Conserved residues within the RKIP (PEBP) family. (b) Conserved residues within the Bax family. (c) Conserved residues within the EEA1 family. (d) Conserved residues within the Troponin I family.

Table S1. Data collection and refinement statistics for RKIP wt and the His-RKIP^{Δ143-6} variant.

Data collection	Wild-type RKIP	RKIP^{Δ143-6}
Wavelength	0.91841	0.91841
Space group	P2 ₁ 2 ₁ 2 ₁	I23
Unit cell parameters		
a/b/c (Å)	32.58 / 54.09 / 97.95	111.25/ 111.25/ 111.25
Resolution (Å)	23.06 - 1.3	55.63 – 2.66
Total reflections	172197	81287
Unique reflections	42630 (6048)	6706 (965)
Completeness (%)	98.5 (97.3)	100 (100)
Redundancy	4.0 (4.0)	12.1 (11.5)
R _{merge} (%)	8.2 (64.4)	10.6 (146.5)
R _{pim} (%)	4.6 (36.6)	3.2 (45.0)
<I/σ(I)>	8.6 (2.0)	14.7 (1.8)
Refinement		
Total number of atoms	1717	1404
Protein	1451	1396
Water molecules	250	6
Glycerol	2	-
Acetate	1	-
Zn	-	1
Cl	-	1
R _{cryst} (%) ²	12.48	20.96
R _{free} (%) ²	16.81	25.04
r.m.s.d. from ideal values in		
Bond lengths (Å) ²	0.011	0.009
Bond angles (°)	1.559	1.322
Planar groups (Å)	0.008	0.005
Chiral centers (Å ³)	0.106	0.078
Coordinate error (Å)	0.035	0.293
Average B-values (Å ²)		
Protein	15.60	87.14
Water	27.54	70.71
Glycerin	28.57	-
Acetate	16.42	-
Zn	-	59.82
Cl	-	68.24
Ramachandran plot (favored/allowed/disallowed)	98.55/0.72/0.72	96.34/2.44/1.22
PDB code	5M0F	5M0G

Table S2.**Analysis of Phosphotheft Motif Among Hetero-oligomers on a per complex basis¹**

Parameter ¹	Invertebrates	Vertebrates	Human	All
S/T at interface (Complex)	1790/2344=76.4 ± 0.88	1779/2513=70.8 ± 0.91	1426/2025=70.4 ± 1.01	3569/4857=73.5 ± 0.63
	1068/1419=75.2 ± 1.14	1189/1633=72.8 ± 1.10	980/1376=71.2 ± 1.22	2257/3052=74.0 ± 0.79
Salt bridge at interface (Complex)	1869/2344=79.7 ± 0.83	1893/2513=75.3 ± 0.86	1561/2025=77.1 ± 0.93	3762/4857=77.5 ± 0.60
	1137/1419=80.1 ± 1.06	1277/1633=78.2 ± 1.02	1076/1376=78.2 ± 1.11	2414/3052=79.1 ± 0.74
Both S/T and Salt bridge at interface (Complex)	1026/2344=43.8 ± 1.02	762/2513=30.3 ± 0.92	606/2025=29.9 ± 1.02	1788/4857=36.8 ± 0.69
	637/1419=44.9 ± 1.32	533/1633=32.6 ± 1.16	423/1376=30.7 ± 1.24	1170/3052=38.3 ± 0.88
Phosphotheft Mechanism with one D/E (Complex)	882/2344=37.6 ± 1.00	720/2514=28.6 ± 0.90	553/2025=27.3 ± 0.99	1602/4857=32.9 ± 0.67
	533/1419=37.6 ± 1.28	490/1636=30.0 ± 1.13	389/1376=28.3 ± 1.21	1023/3052=33.5 ± 0.85
Phosphotheft Mechanism with two D/E's (Complex)	144/2344=6.1 ± 0.50	107/2513=4.3 ± 0.40	58/2025=2.9 ± 0.37	251/4857=5.2 ± 0.32
	95/1419=6.7 ± 0.66	80/1633=4.9 ± 0.53	44/1376=3.2 ± 0.47	175/3052=5.7 ± 0.42

¹ Each entry contains two results: the upper one is for all complex structures ± S,D. error, and the lower one is for all complex structures ± relative error that pass a 40% sequence identity cutoff to minimize redundancy within protein families. S.D. is calculated assuming a binomial distribution.

Table S3.
Analysis of Phosphotheft Motif Among Hetero-oligomers on a per residue basis¹

Parameter¹	Invertebrates	Vertebrates	Human	All
<i>S/T anywhere but not at interface</i> <i>(normalized to total number of residues; not at interface in all complexes)</i>	2571447/ 21643739=11.9	1487175/ 10611252=14.0	998990/ 6811633=14.7	4058622/ 32254991=12.6
	1799382/ 14924935=12.1	1194373/ 8402776=14.2	843368/ 5648894=14.9	2993755/ 23327711=12.8
<i>S/T anywhere on surface</i> <i>(Residue)</i>	121342/ 1043735=11.6	109288/ 764972=14.3	85265/ 587353=14.5	230630/ 1808707=12.8
	77031/ 667512=11.5	78634/ 551258=14.3	64087/ 435144=14.7	155665/ 1218770=12.8
<i>S/T anywhere on interface</i> <i>(Residue)</i>	11276/ 90025=12.5	7149/ 49736=14.4	4783/ 35979=13.3	18425/ 139761=13.2
	6636/ 53131=12.5	5323/ 36736=14.5	3585/ 26699=13.4	11959/ 89867=13.3
<i>R/K anywhere but not at interface</i> <i>(Residue)</i>	2249948/ 21643739=10.4	1086342/ 10611252=10.2	718216/ 6811633=10.5	3336290/ 32254991=10.3
	1550733/ 14924935=10.4	857682/ 8402776=10.2	593357/ 5648894=10.5	2408415/ 23327711=10.3
<i>R/K anywhere on surface</i> <i>(Residue)</i>	194023/ 1043735=18.6	142649/ 764972=18.6	110973/ 587353=18.9	336672/ 1808707=18.6
	126232/ 667512=18.9	102391/ 551258=18.6	81832/ 435144=18.8	228623/ 1218770=18.8
<i>R/K anywhere on interface</i> <i>(Residue)</i>	22285/ 90025=24.8	11298/ 49736=22.7	8037/ 35979=22.3	33583/ 139761=24.0
	13191/ 53131=24.8	8316/ 36736=22.6	6011/ 26699=22.5	21507/ 89867=23.9
<i>D/E anywhere but not at interface</i> <i>(Residue)</i>	2589417/ 21643739=12.0	1169997/ 10611252=11.0	788140/ 6811633=11.6	3759414/ 32254991=11.7
	1799721/ 14924935=12.1	928233/ 8402776=11.0	649706/ 5648894=11.5	2727954/ 23327711=11.7
<i>D/E anywhere on surface</i> <i>(Residue)</i>	204152/ 1043735=19.6	138772/ 764972=18.1	109378/ 587353=18.6	342924/ 1808707=19.0
	133400/ 667512=20.0	100335/ 551258=18.2	80594/ 435144=18.5	233735/ 1218770=19.2
<i>D/E anywhere on interface</i> <i>(Residue)</i>	27402/ 90025=30.4	14744/ 49736=29.6	10481/ 35979=29.1	42146/ 139761=30.2
	16379/ 53131=30.8	10761 36736=29.3	7639/ 26699=28.6	27140/ 89867=30.2

¹ Each entry contains two results: the upper one is for all individual residues within the complex, while the lower one is for all individual residues within the complex that pass a 40% sequence identity cutoff to minimize redundancy within protein families.

Table S4. PEBP species exhibiting conservation of S153 *Homo sapiens*

Pan troglodytes

Gorilla gorilla

Callithrix jacchus

Pongo abelii

Chlorocebus sabaeus

Macaca mulatta

Macaca fascicularis

Papio anubis

Tupaia chinensis

Loxodonta africana

Bos taurus

Felis catus

Ovis aries

Mustela putorius furo

Ailuropoda melanoleuca

Sus scrofa

Otolemur garnettii

Equus caballus

Cavia porcellus

Desmodus rotundus

Canis lupus familiaris

Myotis lucifugus

Neovison vison

Camelus ferus

Rattus norvegicus

Nipponia nippon

Chaetura pelagica

Alligator mississippiensis

Amazona aestiva

Nomascus leucogenys

Aptenodytes forsteri

Picoides pubescens

Oreochromis niloticus

Gasterosteus aculeatus

Larimichthys crocea

Takifugu rubripes

Myotis brandtii

Xenopus laevis

Xenopus tropicalis
Astyanax mexicanus
Danio rerio
Pygoscelis adeliae
Pipa carvalhoi
Pelecanus crispus
Calypte anna

Table S5. Bax species exhibiting conservation of phosphotheft motif *Homo sapiens*

Macaca fascicularis

Chlorocebus sabaeus

Macaca mulatta

Otolemur garnettii

Bos mutus

Mustela putorius furo

Capra hircus

Bos taurus

Canis lupus familiaris

Ictidomys tridecemlineatus

Sus scrofa

Felis catus

Callithrix jacchus

Papio anubis

Ailuropoda melanoleuca

Gorilla gorilla gorilla

Heterocephalus glaber

Cavia porcellus

Pteropus alecto

Rattus norvegicus

Ovis aries

Mus musculus

Cricetulus griseus

Oryctolagus cuniculus

Tupaia chinensis

Camelus ferus

Monodelphis domestica

Fukomys damarensis

Pongo abelii

Myotis lucifugus

Pan troglodytes

Nomascus leucogenys

Loxodonta africana

Bubalus bubalis

Mesocricetus auratus

Equus caballus

Alligator mississippiensis

Anolis carolinensis

Xenopus tropicalis

Myotis davidii

Xenopus laevis

Taeniopygia guttata

Table S6. EEA1 species exhibiting conservation of phosphotheft motif *Homo sapiens*

Sarcophilus harrisii

Equus caballus

Bos mutus

Gorilla gorilla gorilla

Mustela putorius furo

Papio anubis

Pongo abelii

Oryctolagus cuniculus

Neovison vison

Felis catus

Macaca fascicularis

Macaca mulatta

Nomascus leucogenys

Chlorocebus sabaeus

Pan troglodytes

Otolemur garnettii

Callithrix jacchus

Ictidomys tridecemlineatus

Pteropus alecto

Sus scrofa

Loxodonta africana

Heterocephalus glaber

Cricetulus griseus

Tupaia chinensis

Myotis davidii

Fukomys damarensis

Desmodus rotundus

Canis lupus familiaris

Rattus norvegicus

Ailuropoda melanoleuca

Ovis aries

Ornithorhynchus anatinus

Fulmarus glacialis

Myotis lucifugus

Myotis brandtii

Mus musculus

Monodelphis domestica

Cavia porcellus

Alligator mississippiensis
Phaethon lepturus
Phalacrocorax carbo
Gallus gallus
Meleagris gallopavo
Eurypyga helias
Pterocles gutturalis
Pygoscelis adeliae
Cathartes aura
Mesitornis unicolor
Tyto alba
Calypte anna
Anas platyrhynchos
Pelecanus crispus
Nestor notabilis
Ficedula albicollis
Taeniopygia guttata
Nipponia nippon
Pelodiscus sinensis
Amazona aestiva
Balearica regulorum gibbericeps
Manacus vitellinus
Egretta garzetta
Aptenodytes forsteri
Chlamydotis macqueenii
Cuculus canorus
Tinamus guttatus
Opisthocomus hoazin
Struthio camelus australis
Danio rerio
Podiceps cristatus
Acanthisitta chloris
Charadrius vociferus
Ophiophagus hannah
Crotalus horridus
Anolis carolinensis
Lepisosteus oculatus
Latimeria chalumnae
Astyanax mexicanus
Larimichthys crocea

Takifugu rubripes
Oryzias latipes
Gasterosteus aculeatus
Tetraodon nigroviridis
Poecilia formosa
Xiphophorus maculatus
Scleropages formosus
Fundulus heteroclitus
Ictalurus punctatus
Oreochromis niloticus
Oncorhynchus mykiss
Xenopus tropicalis
Callorhynchus milii

Table S7. Troponin I species exhibiting conservation of phosphothreonine motif *Homo sapiens*

Nomascus leucogenys

Pongo abelii

Chlorocebus sabaeus

Pan troglodytes

Macaca fascicularis

Macaca mulatta

Callithrix jacchus

Canis lupus familiaris

Sus scrofa

Ailuropoda melanoleuca

Mustela putorius furo

Cavia porcellus

Felis catus

Ictidomys tridecemlineatus

Mus musculus

Heterocephalus glaber

Rattus norvegicus

Otolemur garnettii

Oryctolagus cuniculus

Tupaia chinensis

Bos taurus

Bos mutus

Ovis aries

Equus caballus

Capra hircus

Papio anubis

Neovison vison

Monodelphis domestica

Anolis carolinensis

Rhinella marina

Xenopus laevis

Alligator mississippiensis

Xenopus tropicalis

Lithobates catesbeiana

Latimeria chalumnae

Meleagris gallopavo

Gallus gallus
Coturnix coturnix japonica
Gorilla gorilla gorilla
Lepisosteus oculatus
Ophiophagus hannah
Danio rerio
Callorhinchus milii
Oncorhynchus mykiss
Esox lucius
Anas platyrhynchos
Picoides pubescens
Sarcophilus harrisii
Salmo salar
Ficedula albicollis
Gasterosteus aculeatus
Balearica regulorum gibbericeps
Cathartes aura
Egretta garzetta
Haliaeetus albicilla
Tinamus guttatus
Cuculus canorus
Loxodonta africana
Coturnix coturnix
Fukomys damarensis
Tauraco erythrolophus
Fulmarus glacialis
Gavia stellata
Manacus vitellinus
Phoenicopiterus ruber ruber
Nipponia nippon
Charadrius vociferus
Pygoscelis adeliae
Tyto alba
Corvus brachyrhynchos
Pelecanus crispus
Podiceps cristatus
Taeniopygia guttata
Pelodiscus sinensis

Buceros rhinoceros silvestris
Struthio camelus australis
Phalacrocorax carbo
Astyanax mexicanus
Oreochromis niloticus
Opisthocomus hoazin
Nestor notabilis
Fundulus heteroclitus
Scleropages formosus
Dicentrarchus labrax
Camelus ferus
Poecilia formosa
Xiphophorus maculatus
Oryzias latipes
Takifugu rubripes
Tetraodon nigroviridis
Poeciliopsis prolifica
Ictalurus punctatus
Larimichthys crocea
Myotis davidii
Amazona aestiva
Anoplopoma fimbria
Pelodytes ibericus
Ictalurus furcatus
Antrostomus carolinensis
Halocynthia roretzi
Ciona intestinalis
Campylomormyrus compressirostris
Ciona savignyi
Polyandrocarpa misakiensis
Chelyosoma siboja
Phaethon lepturus
Merops nubicus
Pimephales promelas
Clupea harengus